Appl Phys B (2011) 102: 141–147
DOI 10.1007/s00340-010-4188-2

Applied Physics B
Lasers and Optics

Effects of O_2–CO_2 polarization beating on femtosecond coherent anti-Stokes Raman scattering (fs-CARS) spectroscopy of O_2

W.D. Kulatilaka · J.R. Gord · S. Roy

Received: 10 April 2010 / Revised version: 23 July 2010 / Published online: 15 September 2010

Abstract Femtosecond coherent anti-Stokes Raman scattering (fs-CARS) spectroscopy has recently emerged as a promising laser-based temperature-measurement technique in flames. In fs-CARS, the broad spectral bandwidths of the pump and Stokes lasers permit the coupling of each ro-vibrational Raman transition via a large number of pump-Stokes photon pairs, creating a strong Raman coherence. However, the broad-bandwidth fs pulses also excite other molecular transitions that are in resonance. The polarization beating between these closely spaced Raman transitions can affect the coherence dephasing rate of the target molecule, making it difficult to extract accurate medium temperature. In a previous study our group investigated N_2/CO polarization beating in N_2 fs-CARS; in the present work we study O_2/CO_2 polarization beating in O_2 fs-CARS. O_2 fs-CARS can be particularly important for thermometry in non-air-breathing combustion in the absence of N_2. The effects of O_2/CO_2 polarization beating are investigated in the temperature range 300–900 K at atmospheric pressure and also at 300 K for pressures up to 10 bar. Unlike in the N_2/CO system, it was observed in the O_2/CO_2 system that the presence of CO_2 can significantly alter the time evolution of the Raman coherence and, hence, affect the measured temperature.

W.D. Kulatilaka (✉) · S. Roy
Spectral Energies, LLC, 5100 Springfield Street, Suite 301,
Dayton, OH 45431, USA
e-mail: waruna.kulatilaka@wpafb.af.mil
Fax: +937-6564110

J.R. Gord
Air Force Research Laboratory, Propulsion Directorate,
Wright-Patterson AFB, OH 45433, USA

1 Introduction

Combustion is the primary energy-conversion process that takes place in almost all heat engines. Combustion chambers of modern engines often involve high-pressure, high-temperature reaction zones with turbulent mixing, where numerous chemical-reactions-dominated instabilities develop, grows, and interact at frequencies of 1–10 kHz or greater. Spatially and temporally resolved temperature and species-concentration measurements in such reaction zones can provide extremely valuable data for validating multi-dimensional turbulent combustion models that can then be utilized to optimize the combustion and energy-transfer processes and to minimize the formation of harmful pollutants in such devices [1]. In recent years femtosecond-laser-based, coherent anti-Stokes Raman scattering (fs-CARS) spectroscopy has emerged as a promising technique for measuring temperature and major-species concentration in turbulent reacting flows at a rate of 1 kHz or greater [2–9].

In fs-CARS thermometry, the frequency difference between two fs laser beams (pump and Stokes) is tuned to a vibrational transition of the target molecule for creating a Raman polarization in the medium. The broad frequency bandwidth of the fs pump and Stokes pulses coherently excites multiple ro-vibrational transitions impulsively. These transitions then begin to oscillate in phase at time zero. However, because of the frequency spread between multiple excited transitions, the Raman coherence dephases over time. The initial dephasing rate is independent of collisions and the Stark shift, two factors which significantly complicate the interpretation of ns-CARS data, but is highly sensitive to temperature [4]. A third laser beam (probe) is scattered off from this Raman polarization and can be used to map the temporal evolution of the Raman coherence. Either a short-pulse probe beam is scanned in time for time-resolved

measurements [2–4, 10, 11] or a chirped probe beam is used to map the initial dephasing, enabling single-shot measurements [7, 12]. In the former method, the temperature is extracted by theoretically fitting the slope of the temporally resolved fs-CARS signal [4, 5]; in the latter, the temperature is extracted by theoretically simulating and fitting the modulation pattern that is recorded using a spectrometer and a CCD camera [7].

In fs-CARS the broad bandwidth of the pump and Stokes pulses contributes to the creation of a strong Raman coherence in the medium that results from the large number of resonant photon pairs [6]. Therefore, single-shot measurements can be readily achieved with a substantial increase in the signal-to-background ratio over that possible with ns-CARS [7]. However, the increased laser bandwidth can simultaneously excite other species that have nearby Raman transitions; hence, the observed CARS signal may consist of interference beatings between various Raman transitions, which complicates the interpretation of the measured CARS signal [13–17]. In this case, the temporally resolved fs-CARS signal recorded will consist of a modulation pattern that results from the beating between the two or more Raman polarizations involved. For example, simultaneous excitation of the CO molecule (Raman shift: 2145 cm^{-1}) while performing N_2 (Raman shift: 2330 cm^{-1}) fs-CARS was the subject of a detailed investigation that was performed previously in our laboratory [2]. It was shown that in the N_2/CO system, the presence of CO has no effect on the *initial* overall coherence dephasing rate and, thus, no effect on the extracted temperature. The presence of CO was manifested only in the oscillations because of the beating between the N_2 and CO Raman polarizations. Furthermore, it was shown that the modulation depth of the beat pattern corresponds to the relative CO/N_2 ratio and, hence, can be used to extract the relative concentration of CO in the medium.

In the current work, we have extended the study of polarization beating that results from the broad-bandwidth fs excitation of the CO_2 molecule in O_2 fs-CARS. O_2 CARS has been developed as a thermometric technique and can be especially important in oxy-fuel combustion where pure O_2 rather than air is used in the oxidizer stream [18]. Oxy-fuel combustion has drawn the attention of combustion researchers for a long time because of its better heat-transfer characteristics, greater flame stability, reduced exhaust gas volume, and decreased levels of pollutants [19]. For example, increased flame temperatures that reach 3000 K or above in oxygen-enhanced combustion become critical in industrial applications such as glass, aluminum, iron, and steel melting [20]. Furthermore, replacing the majority of the N_2 in the inlet air (along with or in the presence of the) increased flame temperatures can virtually eliminate the formation of NO_x in these systems [19]. More recently, clean coal technologies developed for carbon sequestration require that N_2 in the inlet gas be replaced by recycled CO_2 in the combustion of pulverized coal [21]. Oxy-fuel combustion will likely have wider applications in the near future because of advances in noncryogenic-membrane-separation technologies for cost effective generation of O_2 [22]. In these combustion systems, O_2 becomes the candidate of choice for CARS-based thermometry.

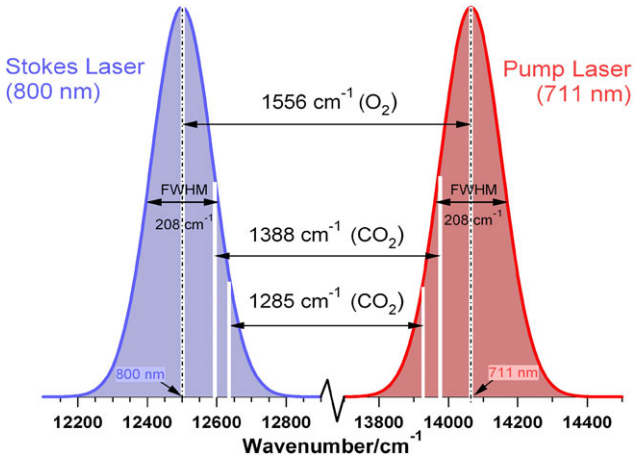

Fig. 1 Simultaneous excitation of O_2–CO_2 Raman bands. The pulse widths shown correspond to Fourier-transform-limited bandwidths of 80-fs pulses

In fs-CARS of O_2, while the O_2 Raman transition is excited at 1556 cm^{-1}, Fermi dyads of CO_2 at 1285 cm^{-1} and 1388 cm^{-1} will be simultaneously excited because of the broad bandwidths of the pump and Stokes lasers [23–25]. The simultaneous excitation of O_2 and CO_2 Raman transitions is illustrated schematically in Fig. 1. Unlike in the N_2/CO system where the two diatomic molecules involved are nearly identical in mass and molecular structure, in the O_2/CO_2 system the two molecules involved in the Raman polarization beating are different. Also the involvement of two CO_2 Fermi dyads and the resulting beating between three Raman polarizations can further complicate the time-resolved CARS signal. Therefore, it is important to investigate the O_2/CO_2 polarization beatings in O_2 fs-CARS and their effects on the resulting coherence dephasing rate and, hence, the extracted temperature. In the present work we performed a detailed investigation of O_2/CO_2 polarization beatings up to 900 K at 1-bar pressure and also at room temperature for pressures up to 10 bar. Time-resolved fs-CARS was employed to investigate the coherence decay rate during the first few picoseconds (typically $<$10 ps) after the impulsive excitation. The results indicate that the presence of CO_2 in substantial quantities can affect the temperature measurement from O_2 fs-CARS. The experimental apparatus and the procedure are described in Sect. 2. The results of O_2/CO_2 polarization beatings investigated using temporally resolved fs-CARS are presented in Sect. 4, along with a the-

oretical explanation of the observed beat patterns. The final section contains some concluding remarks.

2 Experimental apparatus and procedure

The experimental apparatus used for the current study is similar to that used in our previous fs-CARS studies [2–4]. A Ti:sapphire regenerative amplifier (Coherent, Inc., Model: Libra) was operated at 1 kHz to generate ~1 mJ of 800-nm output with an 85-fs pulse duration, full-width at half-maximum (FWHM). Approximately 120 μJ of this output was used for the Stokes beam, and the remainder was employed to pump an optical parametric amplifier (OPA) (Coherent, Inc., Model: OPeRA Solo). The frequency-doubled OPA output was centered at ~712 nm for O_2 fs-CARS. The peak energy of the doubled output was ~50 μJ, which was split in half to form pump and probe beams for the CARS process. The spectral width (FWHM) of the Stokes beam was ~165 cm^{-1} and that of the pump/probe beams was ~380 cm^{-1} at 712-nm. The probe-beam channel included a 15-cm physical delay to permit the probe beam to be delayed temporally with respect to the pump and Stokes beams. The CARS signal was transmitted through a bandpass filter and detected by a photodetector (New Focus, Model:2051) that was connected to a lock-in amplifier, which was modulated at 1 kHz using the trigger output from the regenerative amplifier as the source of the local oscillator. The lock-in time constant was set at 300 ms, and the sensitivity was adjusted through computer control according to the amplitude of the input signal. Measurements were performed in a heated gas cell that was placed at the CARS probe volume. The gas-cell temperature can be adjusted between 300 K and 900 K, with ±2 K precision at a total pressure of 1 bar. At room temperature the gas cell can also be pressurized up to 10 bar. The gas cell was filled with high-purity O_2, CO_2, or calibrated O_2/CO_2 mixtures during the experiment. Different O_2/CO_2 mixtures were prepared, based on the partial pressures after the gas cell had been completely evacuated.

The time evolution of the Raman coherence generated by the pump and Stokes pulses was probed by physically scanning the delay of the probe beam. The coherence dephasing rate can be mapped using the fs-CARS signal decay rate that is recorded as a function of the probe delays. The probe-delay translation stage has a total scan range of 150 mm with a minimum step size of 0.5 μm, which corresponds to a time step of 3.33 fs in the folded-double-pass configuration, and a unidirectional repeatability that is better than 1.5 μm. In general, the probe scan step size was fixed at 2 μm, which corresponds to 13.3 fs in time. Each scan was repeated at least three times. The photodetector gain was set at 1×10^3, and the output signal was maintained below 5 mV in all cases, which was determined to be the upper limit for the linear response range of the detector. The lock-in time constant was set at 300 ms for all measurements. Scattered light detected by the photodetector was maintained at negligible levels to eliminate the need for signal background correction.

3 Results and discussion

Figure 2 shows the peak-normalized, time-resolved fs-CARS signals that were recorded for approximately the first 8 ps after the impulsive excitation by scanning the probe time delay. The solid lines show the fs-CARS signal recorded for $T = 300$, 500, 700, and 900 K for pure O_2. The probe time delay of 0 ps corresponds to the position where the maximum signal was observed on the photodetector; in this position, which is referred to as the coherence spike, the pump, Stokes, and probe beams are perfectly overlapped in time. The strong dependence of the O_2 initial coherence dephasing rate on the cell temperature verifies that O_2 is a good candidate for collision-free temperature measurements in gaseous flows. As shown in Ref. [4], by theoretically fitting this signal decay rate, one can extract the temperature of the medium accurately. Also the dotted lines in Fig. 2 show the signal decay rates recorded at each cell temperature when 10% CO_2 was present in the medium. In this temperature range the presence of 10% CO_2 does not cause any noticeable change in the coherence dephasing rates and, hence, is unlikely to cause deviations in the temperature extracted using the O_2 fs-CARS model. This is particularly advantageous since the spectroscopy of a triatomic molecule such as CO_2 can be significantly more complicated than that of diatomic molecules [23, 24].

However, in many practical hydrocarbon-fueled combustors, the ratio of CO_2 to O_2 can reach well above 1:10, particularly in post-flame regions. For example, during oxy-fuel combustion in liquefied-natural-gas (LNG)-fired combustors, the ratio of CO_2 to O_2 can reach as much as 10:1 or

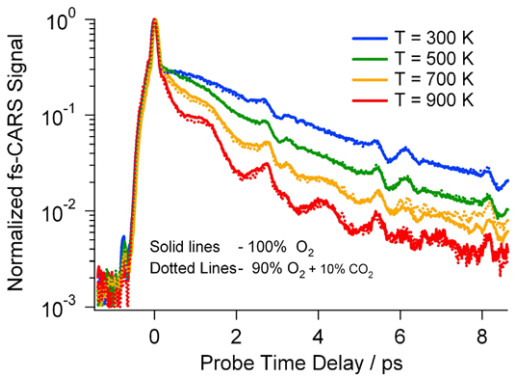

Fig. 2 Initial CARS signal decay recorded by delaying the probe beam with respect to the pump and Stokes beams for gas-cell temperatures ranging from 300 to 900 K. The *solid lines* represent the signals with pure O_2, while the *dotted lines* correspond to signals when 10% CO_2 was added to O_2. All curves are peak-normalized at zero probe time delay

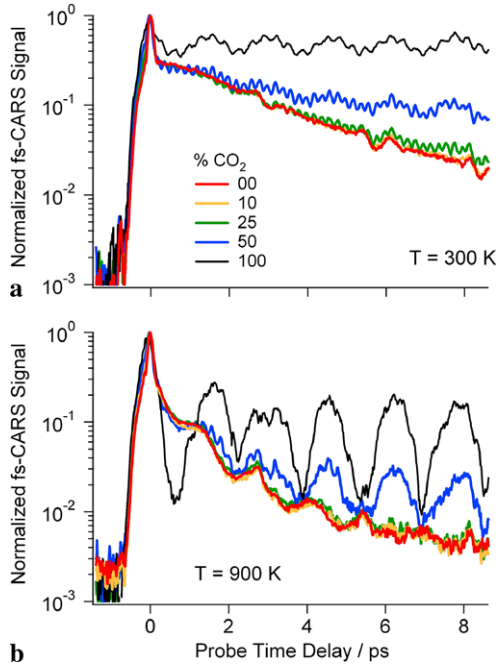

Fig. 3 Initial Raman coherence dephasing recorded while varying the CO_2 percentage in the mixture of O_2/CO_2 at (**a**) $T = 300$ K and (**b**) $T = 900$ K

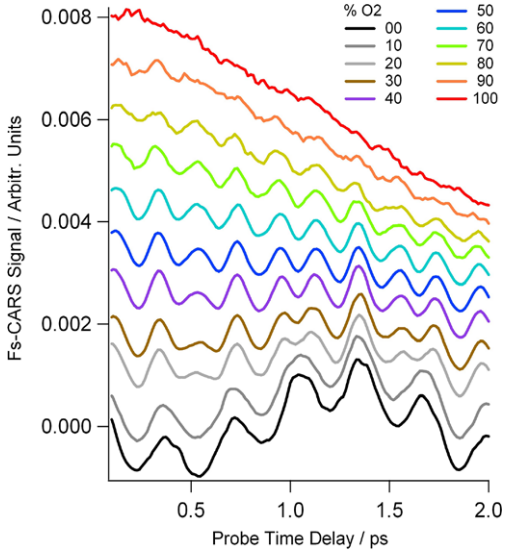

Fig. 4 Initial Raman coherence dephasing at $T = 300$ K and $P = 1$ bar recorded while gradually increasing the CO_2 percentage in the mixture of O_2/CO_2 from 0 to 100%. The profiles are shifted vertically for clarity

higher in parts of the flame [20]. In another example, modern clean coal technologies for carbon capture require that N_2 be replaced by CO_2 in the inlet gas, which results in a significant increase in the CO_2 mole fraction in the reaction zone and the exhaust stream [21]. Therefore it is necessary to investigate the effect of the presence of higher quantities of CO_2 on O_2 fs-CARS thermometry for practical combustion applications. Probe-delay scans similar to those shown in Fig. 2 were repeated in the temperature range 300–900 K while varying the percentage of CO_2 in O_2 from 0% to 100%. The results at $T = 300$ K and $T = 900$ K are shown in Figs. 3(a) and 3(b), respectively. In Fig. 3(a), one can observe that when the CO_2 percentage is increased to 25% at 300 K, a modulation beating between the two molecular resonances occurs as well as a reduction in the slope of the dephasing rate after ~4 ps probe time delay. At the 50% CO_2 level, the modulation due to polarization beating becomes more pronounced, and the signal decay rate changes significantly as compared to that of pure O_2. With pure CO_2 (i.e., no oxygen present), the temporal evolution of the Raman coherence exhibits a very systematic beating pattern, with multiple beat modes overlapping. In this case the overall signal remains nearly constant within the first 8 ps. As shown in Fig. 3(b), at $T = 900$ K, the overall decay rate decreases with an increase in the percentage of CO_2, as compared to the $T = 300$ K case. The signal decay rates appear to be nearly unchanged in the presence of up to 25% CO_2. However, the amplitude of the slower oscillatory beat frequency has increased significantly, as compared to that of the lower temperature case. From these observations it is evident that accurate temperature cannot be extracted simply by mapping the O_2 fs-CARS signal decay at these elevated CO_2 levels. The spectroscopy of O_2 and CO_2 must be included in the fs-CARS model by calculating the modulation beatings between the O_2 and CO_2 Raman coherences. Development of such a model is a challenging task since the spectroscopy of a triatomic molecule such as CO_2 is rather complicated and the relevant spectroscopic parameters such as the J-dependent Raman coherence relaxation rates for CO_2 are not well known. At present, we are involved in an experimental effort to measure directly these relaxation rates using time-resolved ps-CARS [26]. Furthermore, we are updating our single-laser-shot fs-CARS model [7] to include N_2/CO modulation beatings in N_2 fs-CARS. Subsequent work will be focused on the more complicated O_2/CO_2 system.

Beating between O_2 and CO_2 Raman coherences was investigated in greater detail while gradually increasing the presence of CO_2 in O_2 at $T = 300$ K, as shown in Fig. 4. In each mixture composition, the probe-delay scan was repeated five times; the averaged fs-CARS signal is shown. The signals are shifted vertically for clarity. As expected, pure O_2 Raman coherence dephasing does not exhibit any significant beating pattern during this time period. As the CO_2 percentage is increased, the beating modes gradually appear; and at a CO_2 level around ~40%, a very systematic, low-amplitude beating pattern can be observed. As the CO_2 percentage is increased further, several other beating modes begin to appear. At 100% CO_2, the beating patterns consist of two beat frequencies and are consistent with those shown in Fig. 3(a). In an attempt to identify the beating coherences, a simple model was used to predict the individual

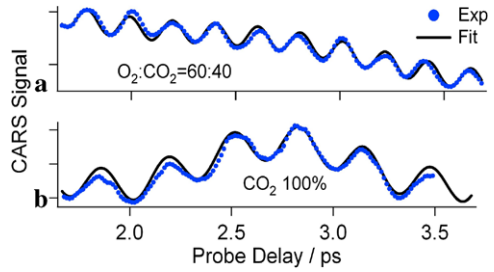

Fig. 5 The Raman coherence dephasing curves for (**a**) 60% $O_2 + 40\%$ CO_2 and (**b**) pure CO_2, as shown in Fig. 4. The *symbols* correspond to experimental data, and the *solid lines* correspond to theoretical fits as described in the text

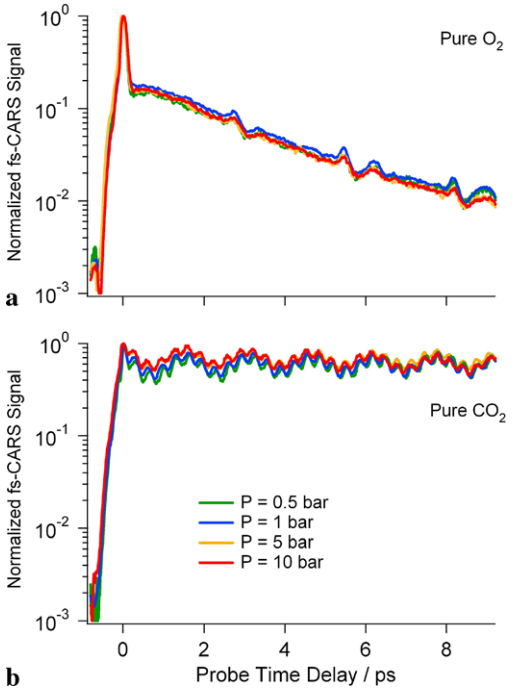

Fig. 6 The time-resolved CARS signal for (**a**) pure O_2 and (**b**) pure CO_2 at $T = 300$ K recorded for gas-cell pressures ranging from 0.5 to 10 bar. All curves are peak-normalized at zero probe time delay

beat frequencies. The beat frequency of two sinusoidal oscillations contains frequency components equal to the sum and the difference of two individual frequencies. In the case of the Raman resonances considered here, the sum frequency component corresponds to the sum of the two Raman frequencies involved (in the GHz frequency range) and, hence, is not detected by our detection system. The difference frequency component is responsible for the rise in the observed beat pattern, as shown in Fig. 4.

As an example, the Raman polarization beating pattern in the case of 40% CO_2 in Fig. 4 can be modeled very well using a sinusoidal oscillation with a frequency of $\sim$163 cm^{-1} that is superpositioned with a linear decay, as shown in Fig. 5(a). The linear decay accounts for the overall dephasing of the Raman coherence due to the large number of slightly out-of-phase oscillations in the vibration-rotation manifold of O_2 [4]. The frequency of the sinusoidal oscillation corresponds closely to the frequency difference between the O_2 Raman shift at 1556 cm^{-1} and the CO_2 Fermi dyad at 1388 cm^{-1}. It should also be noted that compared to the CO_2 Fermi dyad at 1285 cm^{-1}, the one at 1388 cm^{-1} is closer to the frequency difference of the pump and Stokes lasers, which was set at 1556 cm^{-1} during these measurements. Therefore, we conclude that the oscillations observed at lower CO_2 concentrations arise from the polarization beating between the O_2 Raman band and the CO_2 Fermi dyad at 1388 cm^{-1}.

When the CO_2 percentage is increased above 50%, the beat pattern appears to consist of multiple beating modes, as seen in Fig. 4, indicating that both of the CO_2 Fermi dyads are contributing to the polarization beating. The beat pattern observed at 100% CO_2 can be fitted well using a functional form that consists of the sum of two sinusoidals with frequencies of 100 cm^{-1} and 20 cm^{-1}, as shown in Fig. 5(b). The 100-cm^{-1} frequency is approximately equal to the frequency difference between the two CO_2 Fermi dyads. We expect that the 20-cm^{-1} frequency is associated with beating between the (00^00–10^00) and (01^10–11^10) Raman transitions of CO_2 at around 1400 cm^{-1} [25]. For CO_2 concentrations greater than $\sim$50%, the beat pattern becomes a combination of all of the above beating modes, giving rise to the observed beat patterns in Fig. 4.

The current study of O_2/CO_2 Raman polarization beatings was extended into the high-pressure (0–10 bar) regime, although a detailed pressure scaling study of the O_2/CO_2 fs-CARS scheme was beyond the scope of the current work. During these studies the gas cell was filled with pure O_2, pure CO_2, or a calibrated mixture of O_2/CO_2 at different pressures between 0.5 and 10 bar; and the fs-CARS signal was recorded as a function of the probe-delay time. In Figs. 6(a) and 6(b) show the fs-CARS signals of pure O_2 and pure CO_2 at 300 K for four pressures between 0 and 10 bar. As these two plots show, in both cases the evolution of the Raman coherence up to approximately the first 8 ps after the impulsive excitation is not affected by the total pressure. This observation indeed verifies that the dephasing due to collisions is negligible during the initial coherence decay period and that no correction is required for collisional dephasing or energy transfer in the current approach of fs-CARS [4]. In a different observation, for the pure CO_2 case shown in Fig. 6(b), the non-resonant peak around zero probe time delay becomes significantly less pronounced as compared to that for the pure O_2 case shown in Fig. 6(a), although the non-resonant susceptibilities for O_2 [27] and CO_2 [28] as well as the Raman cross sections [29] are nearly comparable. In this case we expect that the CO_2 non-resonant peak gets somewhat "washed out" by the beating between two CO_2 Fermi dyads whose frequency in the

time domain is within a factor of four compared to the laser pulse width. This effect will be investigated further using our theoretical model.

As opposed to the case of O_2, the CO_2 fs-CARS signal overall decay rate is very small—if not negligible—during the first several picoseconds, as can be observed from Figs. 6(a) and 6(b). This behavior can be explained by considering the rotational line spacing of O_2 and CO_2 molecules. The CO_2 rotational line spacing in both Fermi dyads is <0.01 cm^{-1} [23, 24], whereas the average rotational line spacing of the O_2 $\nu = 0 \leftarrow \nu = 1$ band is ~ 1 cm^{-1} [18]. At the time of the initial impulsive excitation, the various ro-vibrational Raman coherences of each molecule begin to oscillate in phase but become slightly out of phase as a result of the very small frequency differences between the rotational transitions. In the case of CO_2, this frequency difference is very small, resulting in negligibly small initial overall dephasing. This initial overall coherence dephasing rate was observed during our experiments to remain nearly unaffected, even when the temperature of the pure CO_2 gas was increased from 300 K to 900 K at 1 bar. However, the modulation beating between the two CO_2 transitions, (00^00–10^00) and (01^10–11^10), increased with temperature, as observed experimentally from the peak-normalized CO_2 fs-CARS signals at different temperatures. This behavior can also be observed in the pure CO_2 case in Figs. 3(a) and 3(b). It can be explained qualitatively by considering the increase in the upper state populations with temperature in the above two transitions, making them strongly coupled at high temperature. Hence, it is expected that this modulation depth can be used to extract the medium temperature if CO_2 fs-CARS is performed in hydrocarbon combustion environments, particularly in post-flame regions, and will be the subject of a future research effort.

4 Conclusion

In conclusion, the presence of CO_2 at lower concentrations, typically below 10%, does not affect the overall coherence dephasing rate in time-resolved O_2 fs-CARS, and hence, does not need to be taken into account while performing thermometry. However, the presence of CO_2 in larger quantities can change the coherence dephasing rate considerably and, hence, must be included in the fs-CARS model to achieve an accurate temperature measurement. A detailed investigation revealed the different Raman polarizations that contribute to the observed beat patterns in the temperature range 300–900 K. Since multiple CO_2 transitions, including the two Fermi dyads, contribute to the observed beat pattern, the O_2 fs-CARS model for practical combustion applications should include all possible CO_2 transitions within the laser bandwidth. The findings of the current study will be utilized to develop high-bandwidth, collision-free O_2 fs-CARS thermometry, in particular, for applications in non-air-breathing combustion where the commonly used target molecule N_2 is absent in the medium. In a different observation, it appears that the temperature of the medium can also be obtained by performing CO_2 fs-CARS, where the amplitude of the observed modulations scales as a function of the temperature.

Acknowledgements Funding for this research was provided by the Air Force Research Laboratory under Contract Nos. FA8650-09-C-2918 and FA8650-09-C-2001 (Ms. Amy Lynch, Program Manager) and by the Air Force Office of Scientific Research (Drs. Julian Tishkoff and Tatjana Curcic, Program Managers).

References

1. S.R. Turns, *An Introduction to Combustion* (WCB/McGraw Hill, Boston, 2000)
2. S. Roy, D. Richardson, P.J. Kinnius, R.P. Lucht, J.R. Gord, Appl. Phys. Lett. **94**, 144101 (2009)
3. S. Roy, P.J. Kinnius, R.P. Lucht, J.R. Gord, Opt. Commun. **281**, 319 (2008)
4. R.P. Lucht, S. Roy, T.R. Meyer, J.R. Gord, Appl. Phys. Lett. **89**, 251112 (2006)
5. R.P. Lucht, P.J. Kinnius, S. Roy, J.R. Gord, J. Chem. Phys. **127**, 044316 (2007)
6. R.P. Lucht, Science **316**, 207 (2007)
7. S. Roy, W.D. Kulatilaka, D. Richardson, R.P. Lucht, J.R. Gord, Opt. Lett. **34**, 3857 (2009)
8. J.R. Gord, T.R. Meyer, S. Roy, Annu. Rev. Anal. Chem. **1**, 663 (2008)
9. S. Roy, J.R. Gord, A.K. Patnaik, Prog. Energy Combust. Sci. **36**, 280 (2010)
10. T. Lang, K.-L. Kompa, M. Motzkus, Chem. Phys. Lett. **310**, 65 (1999)
11. P. Beaud, H.-M. Frey, T. Lang, M. Motzkus, Chem. Phys. Lett. **344**, 407 (2001)
12. T. Lang, M. Motzkus, J. Opt. Soc. Am. B **19**, 340 (2002)
13. R. Leonhardt, W. Holzapfel, W. Zinth, W. Kaiser, Chem. Phys. Lett. **133**, 373 (1987)
14. G. Knopp, K. Kirch, P. Beaud, K. Mishima, H. Spitzer, P. Radi, M. Tulej, T. Gerber, J. Raman Spectrosc. **34**, 989 (2003)
15. D. Pestov, M.H. Zhi, Z.E. Sariyanni, N.G. Kalugin, A. Kolomenskii, R. Murawski, Y.V. Rostovtsev, V.A. Sautenkov, A.V. Sokolov, M.O. Scully, J. Raman Spectrosc. **37**, 392 (2006)
16. T. Kiviniemi, T. Kiljunen, M. Pettersson, J. Chem. Phys. **125**, 164302 (2006)
17. H. Lotem, R.T. Lynch, N. Bloembergen, Phys. Rev. A **14**, 1748 (1976)
18. T.A. Reichardt, P.E. Schrader, R.L. Farrow, Appl. Opt. **40**, 741 (2001)
19. S.V. Naik, N.M. Laurendeau, Combust. Flame **129**, 112 (2002)
20. H.K. Kim, Y. Kim, S.M. Lee, K.Y. Ahn, Energy Fuels **23**, 5331 (2009)
21. C.R. Shaddix, A. Molina, Proc. Combust. Inst. **32**, 2091 (2009)
22. C.E. Baukal Jr., *Oxygen Enhanced Combustion* (CRC Press, Boca Raton, 1998)

23. V.G. Arakcheev, V.V. Kireev, V.B. Morozov, A.N. Olenin, V.G. Tunkin, A.A. Valeev, D.V. Yakovlev, J. Raman Spectrosc. **38**, 1046 (2007)
24. V.G. Arakcheev, V.V. Kireev, V.B. Morozov, A.N. Olenin, V.G. Tunkin, A.A. Valeev, D.V. Yakovlev, J. Raman Spectrosc. **38**, 1038 (2007)
25. A. Chedin, J. Mol. Spectrosc. **76**, 430 (1979)
26. W.D. Kulatilaka, P.S. Hsu, H.U. Stauffer, J.R. Gord, S. Roy, Appl. Phys. Lett. (2010). doi:10.1063/1.3483871
27. G.J. Rosasco, W.S. Hurst, Phys. Rev. A **32**, 281 (1985)
28. D.R. Snelling, A.A. Sawchuk, T. Parameswaran, Appl. Opt. **32**, 7546 (1993)
29. W.R. Fenner, H.A. Hyatt, J.M. Kellam, S.P.S. Porto, J. Opt. Soc. Am. A **63**, 73 (1973)